Inhibition of a biological sulfide oxidation under haloalkaline conditions by thiols and diorgano polysulfanes

Roman, Pawel; Lipińska, Joanna; Bijmans, Martijn F M; Sorokin, D.; Keesman, Karel J.; Janssen, Albert J H

DOI
10.1016/j.watres.2016.06.003

Publication date
2016

Document Version
Accepted author manuscript

Published in
Water Research

This is an Accepted Author Manuscript of an article published by IWA Publishing in the journal Water Research, available online: http://dx.doi.org/10.1016/j.watres.2016.06.003

Inhibition of a biological sulfide oxidation under haloalkaline conditions by thiols and diorgano polysulfanes

Pawel Roman,*[,a,b] Joanna Lipińska,[b,c] Martijn F.M. Bijmans,[b] Dimitry Y. Sorokin,[d,e] Karel J. Keesman,[b,f] Albert J.H. Janssen[a,g]

[a] Sub-department of Environmental Technology, Wageningen University, P.O. Box 17, 6700 AA Wageningen, the Netherlands

[b] Wetsus, European Centre of Excellence for Sustainable Water Technology, Oostergoweg 9, 8911 MA Leeuwarden, the Netherlands

[c] Faculty of Chemistry, Warsaw University of Technology, Noakowskiego St. 3, 00-664 Warsaw, Poland

[d] Winogradsky Institute of Microbiology, Research Centre of Biotechnology, Russian Academy of Sciences, Prospect 60-let Oktyabrya 7/2, 117811 Moscow, Russia

[e] Department of Biotechnology, Delft University of Technology, Julianalaan 67, 2628 BC Delft, The Netherlands

[f] Biobased Chemistry & Technology, Wageningen University, P.O. Box 17, 6700 AA Wageningen, The Netherlands

[g] Shell Technology Centre Bangalore, RMZ Centennial Campus B, Kundalahalli Main Road, Bengaluru 560 048 India

[*] Corresponding author. Phone: +31 (0)317 483339; fax: +31 (0)317 482108; E-mail address: Pawel.Roman@wetsus.nl. Sub-department of Environmental Technology, Wageningen University, P.O. Box 17, 6700 AA Wageningen, the Netherlands

Abstract

A novel approach has been developed for the simultaneous description of sulfur and sulfate formation from the biological oxidation of hydrogen sulfide (H_2S) using a quick, sulfide-dependent respiration test. Next to H_2S, thiols are commonly present in sour gas streams. We investigated the inhibition mode and the corresponding inhibition constants of six thiols and diorgano polysulfanes on the biological oxidation of H_2S. A linear relationship was found between the calculated IC_{50} values and the lipophilicity of the inhibitors. Moreover, a mathematical model was proposed to estimate the biomass activity in the absence and presence of sulfurous inhibitors. The biomass used in the respiration tests originated from a full-scale biodesulfurization reactor. A microbial community analysis of this biomass revealed that two groups of microorganism are abundant, viz. *Ectothiorhodospiraceae* and *Piscirickettsiaceae*.

1. Introduction

Biological processes to remove hydrogen sulfide (H_2S) from gas streams have become increasingly attractive in recent years as an alternative to physicochemical technologies (Janssen et al. 2009; Schieder et al. 2003). Key drivers to select biotechnological solutions for the treatment of sour gas streams instead of physicochemical processes are the higher H_2S removal efficiencies, lower operational cost and, most importantly, the simpler operating procedures (Cline et al. 2003). After the first commercial applications in the oil and gas industry, the need has arisen to broaden the operating window of these bioprocesses by enabling the removal of thiols next to H_2S as these volatile organosulfur compounds are regularly present in sour natural gas streams.

Thiols are considerably more toxic to sulfur oxidizing bacteria (SOB) than dissolved sulfide (Roman et al. 2015b; van den Bosch et al. 2009). In the presence of oxygen thiols are rapidly oxidized to organic disulfides (Eq. 1) (van Leerdam et al. 2011). Thiols also react with biologically produced sulfur particles to form diorgano polysulfanes (Eq. 2). These organosulfur compounds (with $n > 3$) are unstable and quickly decompose to stable di- and trisulfides (Steudel 2002), according to Eq. 3.

$$2\ RSH + 0.5\ O_2 \rightarrow RS_2R + H_2O \quad (1)$$

$$2\ RSH + S_8 \rightarrow RS_nR + S_x^{2-} + 2\ H^+, \text{ with } n+x = 10 \quad (2)$$

$$2\ RS_nR \leftrightarrow RS_{n-1}R + RS_{n+1}R, \text{ with } n > 3 \quad (3)$$

Diorgano di- and trisulfides are found to be the most predominant organosulfur compounds in a bioreactor operating at haloalkaline conditions (Roman et al. 2015b). Clearly, a better understanding of the toxic effects of these compounds on SOB is of key importance to ensure a stable reactor performance.

It was shown that *Thioalkalivibrio sulfidophilus* is the most dominant SOB in full-scale Thiopaq installations that are operated at haloalkaline conditions, i.e. at pH 9, 1 M

total Na^+ and at a redox potential below -250 mV to ensure sulfur-producing conditions (Sorokin et al. 2012). Based on a complete genome analysis Muyzer et al. (2011) reconstructed a sulfur oxidation pathway in *Tv. sulfidophilus*. In this pathway SOB oxidize sulfide to sulfate via zero-valent sulfur as an intermediate. In the first step *Tv. sulfidophilus* oxidizes sulfide to a polysulfur-containing compound(s), hereafter referred to as $\{S_x\}$. $\{S_x\}$ can be secreted from the periplasm as elemental sulfur globules at low redox conditions or oxidized to sulfate via intermediate sulfite at elevated redox values (Fig. 1). The reactions describing the formation of both products can be written in the following simplified form:

$$HS^- + 0.5\ O_2 \rightarrow 1/8\ S_8 + OH^- \quad (4)$$

$$HS^- + 2\ O_2 \rightarrow SO_4^{2-} + H^+ \quad (5)$$

A more detailed description of the underlying principles of biological sulfide oxidation was presented by Klok et al. (2012).

Reaction kinetics of the biological sulfide oxidation processes can be studied by performing biological oxygen monitoring (BOM) tests, which are based on monitoring the decrease of the dissolved oxygen concentration. Recently it was found that for biomass samples in which representatives of the genus *Thioalkalivibrio* were identified as the dominating SOB, the oxygen consumption rate can be described by two different reaction rates (Roman et al. 2015b). The first and fast rate (R1) is related to the partial oxidation of sulfide to $\{S_x\}$, while the second and much lower rate (R2) is related to the further oxidation of $\{S_x\}$ to sulfate ions (Fig. 1) (Sorokin et al. 2008).

We have also shown that by understanding the inhibition mode for a single thiol, it is possible to model the performance of the biodesulfurization process in lab-scale reactors (Roman et al. 2015b). The aim of the current study is to investigate the inhibitory effects of the most common thiols i.e. MT, ethanethiol (ET), 1-propanothiol (PT) and the products of their chemical oxidation (Eq. 1-3): DMDS, diethyl disulfide (DEDS) and dipropyl disulfide

(DPDS) on the biological oxidation rate of dissolved sulfide. The identified modes of inhibition and the associated kinetic parameters will be used in a set of mathematical equations to describe the prevailing reaction kinetics in integrated systems for the treatment of sulfide and thiols containing gas streams. Several authors have presented kinetic models to characterize the aerobic biological sulfide oxidation process (Mora et al. 2016; Klok et al. 2013; Roosta et al. 2011). However, the inhibition by organic sulfur compounds was never taken into account despite the fact that thiols are a commonly present in sour gas streams (Cui et al. 2009; Lee et al. 2006; Kim et al. 2005). Our mathematical model builds on a genomic model proposed by Muyzer et al. (2011). The presented model can be used as a tool for designing industrial biodesulfurization installations.

2. Materials and methods

2.1. Experimental setup

Respiration tests were performed to assess the kinetic parameters of biological sulfide oxidation and the mode of inhibition by thiols and diorgano polysulfanes (Table 1) in an air-saturated medium. We used a similar setup as described elsewhere (Kleinjan et al. 2005), which consisted of a glass mini-reactor (60 mL) equipped with a magnetic stirrer. The reactor was closed with a Teflon piston to avoid any oxygen ingress. We added stock solutions containing the inhibitors and sulfide to the reactor with a syringe passing through the piston. The sulfide oxidation rate was determined by measuring the oxygen consumption rate with a dissolved-oxygen (DO) sensor (Oxymax COS22D, Endress+Hauser). Signals from the DO sensor were recorded using a multiparameter transmitter (Liquiline CM442; Endress+Hauser, the Netherlands). All experiments were performed at 35 °C (DC10-P5/U thermostat bath, Haake, Germany)(Roman et al. 2015a; Graaff 2012; van den Bosch et al. 2009).

2.2. Medium composition

The reactor medium included a carbonate/bicarbonate buffer of 0.1 M Na_2CO_3 and 0.8 M $NaHCO_3$ (1 M total Na^+). Furthermore, the medium contained 1.0 g K_2HPO_4, 0.20 g $MgCl_2 \times 6\ H_2O$, and 0.60 g urea, each per 1 L of Milli-Q water. A trace elements solution (1 mL L^{-1}) was added as described elsewhere (Pfennig and Lippert 1966). The final pH of the medium was 9 at 35 °C.

2.3. Biomass

In the respiration tests we used biomass sampled from a full-scale gas biodesulfurization installation, located at Industriewater Eerbeek B.V., the Netherlands which is operated at oxygen-limiting conditions and low redox potential values (Janssen et al. 2009).

A sulfur-free biomass suspension was prepared by centrifugation (30 min at 16,000 x *g*) of the sulfide-oxidizing culture followed by a washing step after re-suspending the pellet in the same medium as described in section 2.2.

DNA extraction from biomass samples taken from a full-scale gas biodesulfurization installation were performed as follows. First, the samples were washed twice with a buffer of pH 9 and 0.5 M Na^+ to prevent the occurrence of an osmotic shock. Then, the washing was performed by (1) centrifuging the samples at 20,000 x *g* for 5 min; (2) removal of the supernatant; and (3) addition of fresh buffer and mixing with a vortex to re-suspend the pellet. Afterwards, Total Genomic DNA was extracted from the washed biomass using the PowerBiofilm™ DNA Isolation Kit (MoBio, USA) following the manufacturer's instructions. All the above procedures were performed in duplicate.

For biomass samples from the full-scale gas biodesulfurization installation the 16S rRNA gene profiling was performed as following. Illumina 16S rRNA gene amplicon libraries were generated and sequenced at BaseClear BV (Leiden, the Netherlands). In short,

barcoded amplicons from the V3-V4 region of 16S rRNA genes were generated using a 2-step PCR. 10-25 ng genomic DNA was used as template for the first PCR with a total volume of 50 µl using the 341F (5'-CCTACGGGNGGCWGCAG-3') and the 785R (5'-GACTACHVGGGTATCTAATCC-3') primers appended with Illumina adaptor sequences. PCR products were purified and the size of the PCR products were checked on a Bioanalyzer (Agilent, CA, USA) and quantified by fluorometric analysis. Purified PCR products were used for the 2nd PCR in combination with sample-specific barcoded primers. Subsequently, PCR products were purified, checked on a Bioanalyzer (Agilent, CA, USA) and quantified, followed by multiplexing, clustering, and sequencing on an Illumina MiSeq with the paired-end 250 cycles protocol and indexing. The sequencing run was analyzed with Illumina CASAVA pipeline (v1.8.3) with demultiplexing based on sample-specific barcodes. The raw sequencing data produced was processed by removing the sequence reads of too low quality (only "passing filter" reads were selected) and discarding reads containing adaptor sequences or PhiX control with an in-house filtering protocol. A quality assessment on the remaining reads was performed using the FASTQC quality control tool version 0.10.0.

2.4. Respiration tests

Sulfide-dependent O_2-consumption rates were measured in a thermostated reactor (Section 2.1). The biomass concentration was always kept at 10 mg N L^{-1}, measured as the amount of organic nitrogen oxidized to nitrate by digestion with peroxodisulphate (LCK238, Hach Lange, the Netherlands) in triplicate. The medium with biomass was aerated as described elsewhere (van den Bosch et al. 2009). Measurements commenced after sulfide was injected and lasted for 5 to 14 minutes. All solutions containing sulfurous compounds were freshly prepared before each series of experiments. Methanol was used as a solvent for hydrophobic inhibitors (Table 1), which had no effect on the oxygen consumption rate (data

not shown). For all other inhibitors, we used Milli-Q water as a solvent. In order to prevent any oxidation of thiols all solvents were first purged with 99.99% nitrogen gas for at least 15 min.

A wide range of sulfide concentrations was applied to estimate the kinetic parameters for both biological sulfide oxidation rates (R1 and R2, Fig.1). Sulfide concentrations ranging between 0.02 and 0.3 mM were used to estimate kinetic parameters related to R1. In this concentration range R2 was more or less constant and ranges around its maximum value. Hence, a reliable estimation of its value was not possible. In order to estimate kinetic parameters related to R2 significantly lower sulfide concentrations (0.005 - 0.012 mM) were applied. For these ranges of sulfide concentrations, we experimentally verified that the contribution of chemical sulfide oxidation to biological sulfide oxidation is insignificantly small, and can therefore be neglected.

We performed a series of experiments in the absence of any inhibitor to estimate the maximum biological sulfide oxidation (r_{max}) rate and the associated Michaelis constant (K_M). The sulfide concentration for R1 varied from 0.2 to 4.0 K_M and for R2 from 2.0 to 8.0 K_M to obtain reliable estimates of K_M and r_{max} (Marangoni 2003). The methylene blue method (Cuvette test LCK653, Hach Lange, the Netherlands) was used to verify the sulfide concentration in stock solution. All measurements were performed in triplicate. We performed respiration tests in the presence of an inhibitor to identify the mode of inhibition and the parameters for inhibitors that bind to free enzyme (K_i) and enzyme-substrate complex (K_{ies}). In these tests first the inhibitor was added and then the substrate. Each series of experiments was carried out in duplicate. We tested all inhibitors for both oxidation steps (R1 and R2) at 35 °C with an incubation time between 1 and 60 min to determine the time required for biomass incubation with an inhibitor at a certain concentration.

2.5. Modelling biological sulfide oxidation pathway

A mathematical model for describing the biological sulfide oxidation with SOB has been developed on the basis of material balances for sulfide, $\{S_x\}$ and O_2. It has been assumed that in the absence of inhibitors SOB oxidize sulfide (Eq. 6-7) to $\{S_x\}$ (Eq. 8). The formed $\{S_x\}$ is transformed to sulfate which results in an additional oxygen consumption (Eq. 9).

$$\frac{dc_{HS}}{dt} = -c_b \gamma^{R1} \frac{r_{max}^{R1} c_{HS}}{K_M^{R1} + c_{HS}} \quad (6)$$

$$\frac{dc_{O2}^{R1}}{dt} = -c_b \frac{r_{max}^{R1} c_{HS}}{K_M^{R1} + c_{HS}} \quad (7)$$

$$\frac{dc_{Sx}}{dt} = c_b \gamma^{R1} \frac{r_{max}^{R1} c_{HS}}{K_M^{R1} + c_{HS}} - c_b \gamma^{R2} \frac{r_{max}^{R2} c_{Sx}}{K_M^{R2} + c_{Sx}} \quad (8)$$

$$\frac{dc_{O2}^{R2}}{dt} = -c_b \frac{r_{max}^{R2} c_{Sx}}{K_M^{R2} + c_{Sx}} \quad (9)$$

The superscripts $R1$ and $R2$ refer to the first and second oxidation rate, as shown in Figure 1. The model also includes the endogenous oxygen consumption (r_{eg}) (van den Bosch et al. 2009), which was calculated as follows:

$$\frac{dc_{O2}^{eg}}{dt} = -r_{eg} \quad (10)$$

Biomass growth is not included in the model equations as we assume that it remains constant during the relatively short time frame (<14 min) of the respiration experiments (Roman et al. 2015a). It should be noted that the terms used for describing the sulfide and $\{S_x\}$ consumption rates have the same unit, because sulfide is transformed to $\{S_x\}$. The yield coefficients for sulfide (γ^{R1}, mM HS^- (mM O_2)$^{-1}$) and $\{S_x\}$ consumption (γ^{R2}, mM HS^- (mM O_2)$^{-1}$) account for the conversion of r_{max} for oxygen consumption to sulfide consumption. It is not possible to estimate $\gamma^{R1,R2}$ and $r_{max}^{R1,R2}$ independently, as they always appear as the algebraic product $\gamma \cdot r_{max}$. Therefore, the values for $\gamma^{R1,R2}$ were chosen from the stoichiometric equations 4 and 5 and in, what follows, only $r_{max}^{R1,R2}$ and the affinity constants in Eq. 6-9 were estimated from the experimental data. Furthermore, it is assumed that oxygen is not a limiting factor as the

medium is air-saturated i.e. there is an excess amount of oxygen available and the affinity constant for oxygen-respiring SOB are in the range of a few μM (Zannoni and others 2004). BOM tests with sulfide as substrate showed values of 1.5-2.5 μM O_2 for the representatives of the genus *Thioalkalivibrio* (unpublished results). The general mass balances for the substrates and $\{S_x\}$ are solved for the following range of initial experimental conditions:

$$c_{HS}(0) \in [0.003, 0.3] \quad (11)$$

$$c_{Sx}(0) = 0 \quad (12)$$

$$c_{O2}^{R1}(0) \in [0.01, 0.022] \quad (13)$$

$$c_{O2}^{R2}(0) = 0 \quad (14)$$

Furthermore, c_{HS}, c_{Sx} and c_{O2} are the concentrations (in mM) of sulfide, $\{S_x\}$ and oxygen, respectively. The total oxygen consumption is given by:

$$c_{O2}^{tot} = c_{O2}^{R1} + c_{O2}^{R2} + c_{O2}^{eg} \quad (15)$$

An uncertainty assessment of the predicted model output was performed by using a Monte Carlo simulation technique with parameters sampled from the distribution space of the estimated parameters. For each estimated parameter 100 samples were drawn, leading to 100 sampled parameter vectors. For each vector, we calculated the corresponding model output trajectory. Based upon the 100 model output trajectories, the mean and the time-varying standard deviation of the model output were calculated.

2.6. Estimation of kinetic parameters

We estimated the kinetic parameters in Eq. 6-9 by using a static approach in which a stepwise method was taken to minimize the residual error (Marangoni 2003). Firstly, we estimated r_{max} and K_M from experimental data in the absence of an inhibitor for both R1 and R2. Secondly, the estimated parameters (r_{max} and K_M) were substituted into a modified

233 "Michaelis-Menten" equation that describes the mode of inhibition, to estimate the inhibition
234 constants (K_i and K_{ies}).

235 To estimate the kinetic parameters related to R2, we had to assume the initial sulfide
236 concentrations instead of $\{S_x\}$ concentrations as it is not possible to measure the
237 intracellularly bonded {Sx}. To evaluate the effect of this choice we additionally estimated
238 parameters (r_{max}, K_M, and when applicable the inhibition constants: K_i and K_{ies}) using a
239 dynamic approach which relies on solving the relevant set of differential equations (Eq. 6-10)
240 iteratively. In this approach the $\{S_x\}$ concentration is implicitly calculated from the proposed
241 and validated model (Section 3.4). In particular, we solved the following optimization
242 problem:

243 $$\min \sum(c_{O2}^{tot}(t) - \widehat{c_{O2}^{tot}}(t,\theta))^2 \qquad (16)$$

244 with $\widehat{c_{O2}^{tot}}$ the calculated total oxygen concentration (Eq. 15), given the solutions to Eq. 6-10
245 for the set of kinetic parameters (θ: r_{max}, K_M). In the presence of inhibitors (Eq. 17-19) the set
246 of parameters is extended with the inhibition constants: K_i and K_{ies}. Given the observations of
247 c_{O2}^{tot}, the kinetic parameters were estimated using a non-linear least-squares method
248 (Levenberg-Marquardt algorithm), as described by Keesman (2011).

249

250

251 **3. Results and discussion**

252 ***3.1. Microbial diversity in a full-scale gas biodesulfurization installation***

253 Microbial community analysis of biomass collected from a full-scale gas
254 biodesulfurization installation in Eerbeek (the Netherlands) showed that the bacterial
255 composition (Supplementary Information, Fig. S1) is similar to what has been described
256 previously (Sorokin et al. 2012). The dominant bacterial group (approximately 50% of the
257 16S rRNA sequences analyzed) belongs to the family *Ectothiorhodospiraceae*. Within this

group, 99% of the 16S rRNA sequences belonged to the genus *Thioalkalivibrio* Also bacteria related to the family *Piscirickettsiaceae* are abundant, 24.8% and 26.1% in both replicates. Within this group, approximately 80% of the 16S rRNA sequences are closely related to the *Thiomicrospira pelophila*/*Thioalkalimicrobium* cluster, which are often present in the full-scale Thiopaq installations (Sorokin et al. 2011).

3.2. Determination of incubation time

A complete saturation of enzymes with an inhibitor is required in order to properly determine the inhibition constants (K_i and K_{ies}). Zhang et al. (2001) indicated that in the presence of an inhibitor the incubation time needed to reach complete saturation is related to the inhibitor concentration which, in turn, is related to the degree of inhibition. Due to different susceptibilities of R1 and R2 to the inhibitors (Roman et al. 2015a) it was necessary to apply different inhibitor concentrations, i.e. a higher and a lower one for respectively R1 and R2 (Fig.1). The concentration of each inhibitor was chosen such that only partial inhibition was achieved. An appropriate incubation time for each concentration of each inhibitor had to be determined whilst taking into account that too long incubation times for thiols shall be avoided in order to prevent any chemical oxidation to disulfides (Eq. 1).

From the results shown in Figure 2 it follows that R1 and R2 require different incubation times to reach a complete saturation of the enzymes in the presence of an inhibitor. Table 2 shows the inhibitor concentrations and incubation times that were selected in the remainder of this study.

3.3. Determination of inhibition mode and kinetic parameters

The results from sulfide-dependent respiration tests were plotted in double-reciprocal plots (Supplementary Information, Fig. S2) to identify the inhibition mode related to R1 and

R2. From this plot it clearly follows that MT, ET and PT act as competitive inhibitors for R1. Therefore, the mode of inhibition can be described by a modified "Michaelis-Menten" equation:

$$r_i^{R1} = \frac{r_{max}^{R1} c_{HS}}{K_M^{R1}\left(1+\frac{c_i}{K_i^{R1}}\right)+c_{HS}} \quad (17)$$

where c_i is an inhibitor concentration. This mode of inhibition is in agreement with our previous findings viz. that MT acts as a competitive inhibitor for sulfide oxidation by SOB (Roman et al. 2015a). According to Wilms et al. (1980), this can be explained by the structural similarity between sulfide (HS^-) and MT (CH_3S^-). In contrast, diorgano disulfides are non-competitive inhibitors for R1 and their inhibitory effects can be described as follows:

$$r_i^{R1} = \frac{r_{max}^{R1} c_{HS}}{K_M^{R1}+c_{HS}\left(1+\frac{c_i}{K_{ies}^{R1}}\right)} \quad (18)$$

This type of inhibition is common in multi-substrate reactions (Eq. 4-5) in contrast to single-substrate reactions (Segal 1993).

To establish the effect of thiols and diorgano polysulfanes on R2, double reciprocal plots were prepared which show a mixed type of inhibition (Supplementary Information, Fig. S2), indicating that the inhibitors are able to bind at the active and allosteric site of enzymes. The corresponding specific reaction rate is given by:

$$r_i^{R2} = \frac{r_{max}^{R2} c_{HS}}{K_M^{R2}\left(1+\frac{c_i}{K_i^{R2}}\right)+c_{HS}\left(1+\frac{c_i}{K_{ies}^{R2}}\right)} \quad (19)$$

It is obvious that equations 17-19 only describe a phenomenological characterization of the experimental observation but do not provide any underlying mechanisms. However, in section 3.4, we will describe that the lipophilicity effects of the inhibitors influence the inhibition of sulfide oxidation. Then, the specific reaction rates (Eq. 17-19) can substitute the generic rates mentioned (Eq. 6-9) to predict the biomass activity in the presence of thiols and diorgano polysulfanes.

After unrevealing the mode of inhibition for each inhibitor on R1 and R2, it was possible to estimate the kinetic parameters in equations 17-19. Estimated values of r_{max}, K_M, K_i and K_{ies} and the corresponding standard deviations are shown in Table 3. From these parameter estimations it follows that MT is the most toxic thiol as it has the lowest K_i value. This is in agreement with our hypothesis that the inhibitory effect decreases with increasing steric hindrance of the thiols (Roman et al. 2015a). Estimated values of K_{ies} for R1 and diorgano polysulfanes are strongly correlated with their molecular weight (R^2 = 0.999). Similar strong correlations are observed for K_i and K_{ies} of thiols and for K_i of diorgano polysulfanes for R2. However, K_{ies} of diorgano polysulfanes is more or less constant (approximately 0.24 mM), indicating that the same non-competitive inhibition mechanism applies. Because the diorgano polysulfanes in our tests only differ in their aliphatic chain length while the number of sulfur atoms remains the same, it can be hypothesized that non-competitive inhibition (K_{ies}) is related to the sulfur-sulfur bond.

The results from the parameter estimations show that there is no significant difference between the estimated values obtained via the dynamic and the static approach (data not shown). However, the dynamic approach yields K_m values with a higher level of uncertainty in the estimate because the data contained less information.

3.4. Calculation of IC_{50} and its correlation with lipophilicity

The IC_{50} value represents the inhibitor concentration at which 50% inhibition occurs of an enzymatic reaction at a specific substrate concentration. A mathematical relation between the inhibition constants and the IC_{50} value is described by Yung-Chi and Prusoff (1973). Equations describing this relationship for competitive, uncompetitive and mixed inhibition are given by:

$$IC_{50} = K_i \left(1 + \frac{c_{HS}}{K_M}\right) \quad (20)$$

$$IC_{50} = K_{ies} \left(1 + \frac{K_M}{c_{HS}}\right) \quad (21)$$

$$IC_{50} = \frac{c_{HS} + K_M}{\frac{K_M}{K_i} + \frac{c_{HS}}{K_{ies}}} \quad (22)$$

Based on the estimated values for the kinetic parameters and the corresponding uncertainties (Table 3), we calculated IC_{50} values with uncertainty bounds for both oxygen consumption rates (R1 and R2) and for each of the inhibitors (Fig. 3 A-C). Taking into account that the IC_{50} value is dependent on the substrate concentration, results are plotted in the range of 0-3 mM sulfide. To compare our results with available literature data, the IC_{50} values for MT and DMDS for R1 have been reviewed (Table 4). The values for both inhibitors are very similar to previously reported data. It can be seen that thiols become less toxic with increasing substrate concentrations (Fig. 3A), while the IC_{50} values for diorgano polysulfanes stabilize at around 1 mM for substrate concentrations above 0.5 mM (Fig. 3B). Moreover, it can be observed that R2 is more susceptible to the inhibitors at almost all sulfide concentrations (Fig. 3C) because of much lower IC_{50} values. These results support our previous findings from lab-scale reactor experiments that biological production of sulfate is more vulnerable to inhibitors than the biological production of sulfur (Roman et al. 2015a; Roman et al. 2015b).

It is known that the biological activity of inhibitors can be directly related to their physicochemical properties (Cronin 2004). Hence, we compared their lipophilicity expressed as logarithm of octanol-water partition coefficient (log(P)), with the measured IC_{50} values. The estimation of log(P) for the various inhibitors was calculated using ALOGPS 2.1 software (Anon n.d.; Tetko and Tanchuk 2002). For thiols the log(P) values ranged from 0.4 to 1.2 and for diorgano polysulfanes ranged from 1 to 3. To determine whether lipophilicity is correlated with IC_{50} values at sulfide concentration of 0.2 mM, the relationship between

log(P) and IC_{50} values for the particular group of inhibitors for both oxidation rates (R1 and R2) was assessed by linear regression (Fig. 4 A-B). A clear and positive correlation was found between log(P) and the IC_{50} values for thiols for both R1 and R2, with coefficients of determination of 0.848 and 0.999, respectively (Fig. 4A). These correlations show that hydrophobic thiols are less toxic to SOB compared to the more hydrophilic ones. This might also indicate that inhibition by thiols is related to the hydrophilic interaction in the inhibition mechanisms. For diorgano polysulfanes, we found large negative correlations between log(P) and the IC_{50} values with coefficients of determination of 0.995 and 0.994 for R1 and R2, respectively (Fig. 4B). In contrast to thiols, toxicity of diorgano polysulfanes increases with their lipophilicity which suggests involvement of hydrophobic interaction in the inhibition mechanisms. This could mean that diorgano polysulfanes are affecting enzymes that are embedded in the cell membrane which is in agreement with another observation that diorgano polysulfanes toxicity is not competitive for R1 because the substrate, i.e. sulfide, reacts with enzymes located outside the cell membrane in the periplasm or on the external surface of the cell membrane (Gregersen et al. 2011).

3.5. Comparison of the model results with experimental data

The estimated kinetic parameters in Table 3 were obtained from sulfide-dependent respiration tests and then used in the above described mathematical model (Eq. 6-15). The model predictions were compared with a set of independent respirometric results. The biomass used for the validation experiments was taken from the same full-scale reactor but two months after biomass sampling for the parameter estimation tests.The model was experimentally validated in the absence of an inhibitor with the initial sulfide concentration ranging from 0.005 to 0.2 mM (Fig. 5A-F). From these results, it can be seen that the proposed model predicts the oxygen consumption reasonably well for haloalkaliphilic SOB

cultivated under O_2-limiting conditions. For the highest sulfide concentrations the deviation between experimental measurements and model predictions increases somewhat which can be attributed to a lag phase of the SOB. Nevertheless, an error analysis of r^{R1} showed that the coefficient of variation was always below ± 25%, which is a reasonable margin if one takes into account the measurement errors in the dissolved oxygen, sulfide, biomass concentrations, liquid volumes and influence of the error propagation. Furthermore, the measured and predicted reaction rates seem to correspond (Supplementary Information, Fig. S3). The uncertainty in the model output resulting from uncertainties in the estimates for the kinetic parameters (Table 3) is rather small because of strong correlations between the identifiable parameter estimates, as also follows from the covariance and correlation matrix of the estimates (Supplementary Information, S2). In addition, respiration tests with biomass concentration of 1 mg N L^{-1} were performed to validate the model. Although these tests were performed with ten times lower biomass concentration than tests used for the parameter estimation, no significant differences between the model output and the measured oxygen consumption rate were observed, i.e. the coefficient of variation was below ± 27%.

Hereafter, the model was validated with tests performed at constant initial sulfide concentration (0.03 mM) in the presence of MT, ET and DMDS at different concentrations (Fig. 6A-F). For this purpose, equations describing the model (Eq. 6-15) were adjusted with modified “Michaelis-Menten” equations (Eq. 17-19) depending on the type of inhibitor. For all measurements, model predictions are in a good agreement with the experimental results (on average the difference is 14 ± 4 % for R1 and 7 ± 6 % for R2). This allows for an explicit mathematical description and supports double sulfide-dependent oxygen consumption rates by SOB. Consequently, the model can be used to predict the biomass activity and to predict the accumulation rate of intracellularly produced $\{S_x\}$.

From Figure 6 it can be seen that for biological oxidation of sulfide inhibited by MT and ET, the experimental results and the model predictions show almost two times lower sulfide consumption rates and significantly lower oxidation rates of $\{S_x\}$ compared to uninhibited reactions. For reactions inhibited by DMDS, the oxidation of sulfide is inhibited only slightly (8%, Fig. 6E) and moderately (23%, Fig. 6F), while the oxidation of $\{S_x\}$ is almost completely blocked (Fig. 6E-F). These results clearly show that the sulfide oxidation is significantly less vulnerable to these sulfurous inhibitors than $\{S_x\}$ oxidation is. In the presence of an inhibitor model output uncertainties increased due to the uncertainty of inhibition constants (Figure 5).

4. Conclusions

In this study, a novel approach for the simultaneous description of biological sulfur and sulfate formation using a quick sulfide-dependent respiration test has been presented. By applying approach, the inhibition of haloalkaliphilic SOB by the most common thiols and their corresponding diorgano polysulfanes was described. We found that IC_{50} values are correlated with the lipophilicity of the inhibitors. Thiols interfere with the oxidation of sulfide by hydrophilic interaction while hydrophobic interaction is the most important mechanism for diorgano polysulfanes. This can be related to the ionic and non-ionic form of the various inhibitors. For each inhibitor, we identified the inhibition mode and the corresponding inhibition constants. Understanding the inhibitory properties of thiols on the biological oxidation of sulfide allows designing full-scale systems in which any inhibition is prevented e.g. by increasing the biomass or/and substrate concentration.

Moreover, a mathematical model has been described to calculate the biological sulfide oxidizing capacity in the absence or presence of inhibitory thiols and their corresponding diorgano polysulfanes. The proposed model can be used to design full-scale installations to

remove H_2S from gas streams in which thiols and diorgano polysulfanes are present (Janssen et al. 1998).

Acknowledgements

This work was performed within the cooperation framework of Wetsus, European Centre of Excellence for Sustainable Water Technology (www.wetsus.nl). Wetsus is co-funded by the Netherlands' Ministry of Economic Affairs and Ministry of Infrastructure and the Environment, the European Union's Regional Development Fund, the Province of Fryslân, and the Northern Netherlands Provinces. The authors thank the participants of the research theme "Sulfur" and Paqell for fruitful discussions and financial support.

References

Anon, ALOGPS 2.1 software. Available at: http://www.vcclab.org/lab/alogps [Accessed 2015].

Van den Bosch, P.L.F., de Graaff, M., Fortuny-Picornell, M., van Leerdam, R.C., Janssen, A.J.H., 2009. Inhibition of microbiological sulfide oxidation by methanethiol and dimethyl polysulfides at natron-alkaline conditions. *Appl. Microbiol. Biotechnol.* 83 (3), 579–587.

Cline, C., Hoksberg, A., Abry, R., Janssen, A.J.H., 2003. Biological Process for H2S Removal from Gas Streams: The Shell-Paques/THIOPAQ™ Gas Desulfurization Process. In *Proceedings of the Laurance Reid Gas Conditioning Conference*. p. 1–18.

Cronin, M.T., 2004. *Predicting chemical toxicity and fate*, CRC press.

Cui, H., Turn, S.Q., Reese, M.A., 2009. Removal of sulfur compounds from utility pipelined synthetic natural gas using modified activated carbons. Catal. Today 139 (4), 274–279.

Graaff, C. de, 2012. *Biological treatment of sulfidic spent caustics under haloalkaline conditions using soda lake bacteria*, Thesis Wageningen University.

Gregersen, L.H., Bryant, D.A., Frigaard, N.-U., 2011. Mechanisms and evolution of oxidative sulfur metabolism in green sulfur bacteria. *Front. Microbiol.* 2.

Janssen, A.J.H., Lens, P.N.L., Stams, A.J.M., Plugge, C.M., Sorokin, D.Y., Muyzer, G., Dijkman, H., Van Zessen, E., Luimes, P., Buisman, C.J.N., 2009. Application of bacteria involved in the biological sulfur cycle for paper mill effluent purification. *Sci. Total Environ.* 407 (4), 1333–1343.

Janssen, A.J.H., Meijer, S., Bontsema, J., Lettinga, G., 1998. Application of the redox potential for controling a sulfide oxidizing bioreactor. *Biotechnol. Bioeng.* 60 (2), 147–155.

Keesman, K.J., 2011. *System identification: an Introduction*, Springer, Verlag, UK.

Kim, K.-H., Choi, Y., Jeon, E., Sunwoo, Y., 2005. Characterization of malodorous sulfur compounds in landfill gas. *Atmos. Environ.* 39 (6), 1103–1112.

Kleinjan, W.E., Keizer, A. de, Janssen, A.J., 2005. Kinetics of the chemical oxidation of polysulfide anions in aqueous solution. *Water Res.* 39 (17), 4093–4100.

Klok, J., de Graaff, M., van den Bosch, P.L.F., Boelee, N.C., Keesman, K.J., Janssen, A.J.H., 2013. A physiologically based kinetic model for bacterial sulfide oxidation. *Water Res.* 47(2), 483–492.

Klok, J.B.M., van den Bosch, P.L.F., Buisman, C.J.N., Stams, A.J.M., Keesman, K.J., Janssen, A.J.H., 2012. Pathways of sulfide oxidation by haloalkaliphilic bacteria in limited-oxygen gas lift bioreactors. *Environ. Sci. Technol.* 46 (14), 7581–7586.

Lee, S., Xu, Q., Booth, M., Townsend, T.G., Chadik, P., Bitton, G., 2006. Reduced sulfur compounds in gas from construction and demolition debris landfills. *Waste Manage.* 26

(5), 526–533.

Van Leerdam, R.C., Bosch, P.L.F., Lens, P.N.L., Janssen, A.J.H., 2011. Reactions between methanethiol and biologically produced sulfur. *Environ. Sci. Technol.* 45 (4), 1320–1326.

Marangoni, A.G., 2003. *Enzyme kinetics: a modern approach*, John Wiley & Sons.

Mora, M., López, L.R., Lafuente, J., Pérez, J., Kleerebezem, R., van Loosdrecht, M.C., Gamisans, X., Gabriel, D., 2016. Respirometric characterization of aerobic sulfide, thiosulfate and elemental sulfur oxidation by S-oxidizing biomass. *Water Res.* 89, 282–292.

Muyzer, G., Sorokin, D.Y., Mavromatis, K., Lapidus, A., Clum, A., Ivanova, N., Pati, A., d' Haeseleer, P., Woyke, T., Kyrpides, N.C., 2011. Complete genome sequence of "Thioalkalivibrio sulfidophilus" HL-EbGr7. *Stand. Genomic. Sci.* 4 (1), 23.

Pfennig, N., Lippert, K.D., 1966. Über das vitamin B_{12}-bedürfnis phototropher Schwefelbakterien. Arch. Microbiol. 55 (3), 245–256.

Roman, P., Bijmans, M.F.M., Janssen, A.J.H., 2015a. Influence of methanethiol on biological sulfide oxidation in gas treatment system. *Environ. Tech.* (just-accepted), 1–42.

Roman, P., Veltman, R., Bijmans, M.F.M., Keesman, K., Janssen, A.J.H., 2015b. Effect of methanethiol concentration on sulfur production in biological desulfurization systems under haloalkaline conditions. *Environ. Sci. Technol.* 49, 9212–9221.

Roosta, A., Jahanmiri, A., Mowla, D., Niazi, A., 2011. Mathematical modeling of biological sulfide removal in a fed batch bioreactor. *Biochem. Eng. J.* 58, 50–56.

Schieder, D., Quicker, P., Schneider, R., Winter, H., Prechtl, S., Faulstich, M., 2003. Microbiological removal of hydrogen sulfide from biogas by means of a separate biofilter system: experience with technical operation. *Water Sci. Technol.* 48 (4), 209–212.

Segal, I., 1993. *Enzyme Kinetics: Behavior and Analysis of Rapid Equilibrium and Steady-State Enzyme Systems*, Wiley, New York, USA.

Sorokin, D., van den Bosch, P.L.F., Abbas, B., Janssen, A.J.H., Muyzer, G., 2008. Microbiological analysis of the population of extremely haloalkaliphilic sulfur-oxidizing bacteria dominating in lab-scale sulfide-removing bioreactors. *Appl. Microbiol. Biotechnol.* 80 (6), 965–975.

Sorokin, D.Y., Banciu, H., Robertson, L.A., Kuenen, J.G., Muntyan, M.S., Muyzer, G., 2013. Halophilic and haloalkaliphilic sulfur-oxidizing bacteria. In Rosenberg E. et al., ed. *The Prokaryotes*. Springer-Verlag: Berlin-Heidelberg, p. 529–554.

Sorokin, D.Y., Banciu, H.L., Muyzer, G., 2015. Functional microbiology of soda lakes. Curr. Opin. Microbiol. 25, 88–96.

Sorokin, D.Y., Kuenen, J.G., Muyzer, G., 2011. The microbial sulfur cycle at extremely haloalkaline conditions of soda lakes. *Front. Microbiol.*, 2 (article 44), March 2011.

Sorokin, D.Y., Muntyan, M.S., Panteleeva, A.N., Muyzer, G., 2012. Thioalkalivibrio sulfidiphilus sp. nov., a haloalkaliphilic, sulfur-oxidizing gammaproteobacterium from alkaline habitats. *Int. J. Syst. Evol. Microbiol.* 62 (Pt 8), 1884–1889.

Steudel, R., 2002. The chemistry of organic polysulfanes RS (n)-R (n> 2). Chem. Rev. 102 (11), 3905.

Tetko, I.V., Tanchuk, V.Y., 2002. Application of associative neural networks for prediction of lipophilicity in ALOGPS 2.1 program. *J. Chem. Inf. Comp. Sci.* 42 (5), 1136–1145.

Wilms, J., Lub, J., Wever, R., 1980. Reactions of mercaptans with cytochrome c oxidase and cytochrome c. *Biochim. Biophys. Acta, Bioenerg.* 589 (2), 324–335.

Yung-Chi, C., Prusoff, W.H., 1973. Relationship between the inhibition constant (Ki) and the concentration of inhibitor which causes 50 per cent inhibition (I50) of an enzymatic reaction. *Biochem. Pharmacol.* 22 (23), 3099–3108.

Zannoni, D., others, 2004. *Respiration in archaea and bacteria*, Springer.

Zhang, S., Zhao, H., John, R., 2001. A theoretical model for immobilized enzyme inhibition biosensors. *Electroanalysis* 13 (18), 1528–1534.

TABLES

Table 1. Chemicals used to prepare solutions in the current study. All chemicals were purchased from Sigma-Aldrich, the Netherlands.

Compound name	CAS no.	Chemical formula	Solvent
Sodium sulfide hydrate	1313-84-4	$Na_2S \cdot 9\ H_2O$	Water
Sodium thiomethoxide	5188-07-08	CH_3SNa	Water
Ethanethiol	75-08-1	C_2H_5SH	Methanol
1-Propanethiol	107-03-9	$CH_3CH_2CH_2SH$	Methanol
Dimethyl disulfide	624-92-0	$CH_3S_2CH_3$	Methanol
Diethyl disulfide	110-81-6	$(C_2H_5)_2S_2$	Methanol
Dipropyl disulfide	629-19-6	$(CH_3CH_2CH_2)_2S_2$	Methanol

Table 2. Concentration of inhibitors (C_i) and incubation time (T) used in sulfide-dependent respiration tests for assessing the oxygen consumption rates R1 and R2.

Inhibitor	R1		R2	
	C_i [mM]	T [min]	C_i [mM]	T [min]
Methanethiol	0.024	5	0.005	2
Ethanethiol	0.061	5	0.025	6
Propanethiol	0.080	15	0.017	15
Dimethyl disulfide	0.960	10	0.100	20
Diethyl disulfide	1.200	10	0.100	15
Dipropyl disulfide	0.850	25	0.420	10

570 **Table 3.** Estimated specific maximal reaction rate (r_{max}), Michaelis-Menten constant (K_M) and
571 inhibition constants (K_i and K_{ies}) with their corresponding standard deviation (σ) for the first
572 (R1) and second (R2) oxygen consumption rates.

Reaction rate	Inhibitor	Mode of inhibition	Parameter	Estimated value	σ	Unit
R1 ($HS^- \rightarrow \{S_x\}$)	Not inhibited reaction		r_{max}	600	30	µM O_2 (mg N h)$^{-1}$
			K_M	79	9	µM
	MT	competitive	K_i	23	2	µM
	ET		K_i	46	5	µM
	PT		K_i	50	6	µM
	DMDS	uncompetitive	K_{ies}	1000	90	µM
	DEDS		K_{ies}	710	60	µM
	DPDS		K_{ies}	440	20	µM
R2 ($\{S_x\} \rightarrow SO_4^{2-}$)	Not inhibited reaction		r_{max}	103	4	µM O_2 (mg N h)$^{-1}$
			K_M	1.9	0.4	µM
	MT	mixed	K_i	5	2	µM
			K_{ies}	14	3	µM
	ET		K_i	8.2	0.8	µM
			K_{ies}	40	3	µM
	PT		K_i	10	2	µM
			K_{ies}	70	10	µM
	DMDS		K_i	49	6	µM
			K_{ies}	260	20	µM
	DEDS		K_i	61	6	µM
			K_{ies}	230	20	µM
	DPDS		K_i	100	10	µM
			K_{ies}	220	10	µM

573

574 **Table. 4.** Calculated IC_{50} values for methanethiol and dimethyl disulfide, and comparison
575 with literature data at sulfide concentration of 0.2 mM.

IC_{50} [mM]		**pH**	**$[Na^+ + K^+]$**	**Reference**
Methanethiol	**Dimethyl disulfide**			
0.08 ± 0.01	1.4 ± 0.1	9	1	current study
0.05	1.5	9	2	(van den Bosch et al. 2009)
0.11 ± 0.02	N.A.	8.5	1.5	(Roman et al. 2015a)
0.2 ± 0.6	1.4 ± 0.2	9.5	0.8	(Graaff 2012)

576 N.A. – not available

FIGURES

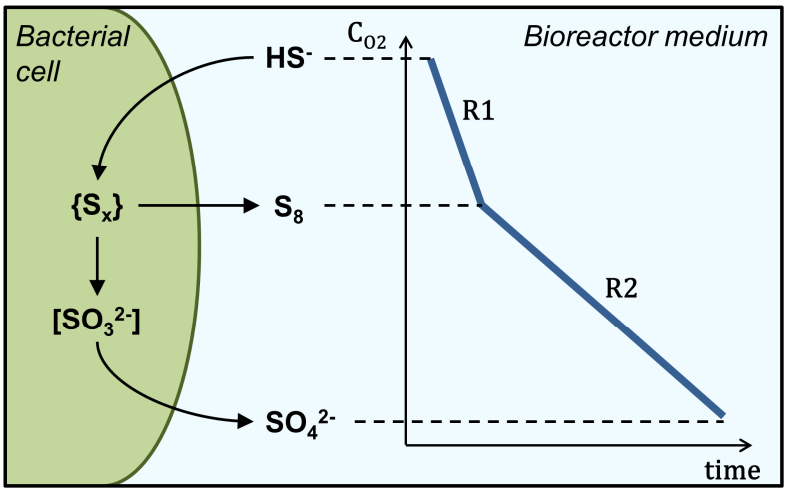

Figure 1. Schematic overview of the reaction that occurs in the bacterial cell related to sulfide oxidation and the corresponding oxygen concentration profile from biological oxygen measurements.

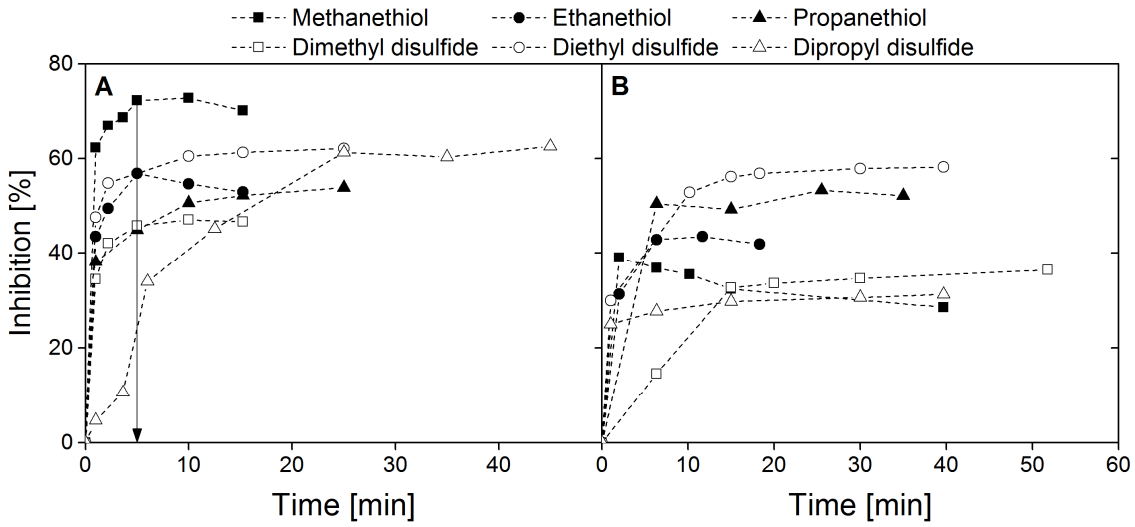

582

583 **Figure 2.** Incubation test performed to investigate time needed for complete saturation of
584 enzymes with inhibitor. **A.** Inhibition results for the first rate of the oxygen consumption rate.
585 Concentrations of methanethiol, ethanethiol, propanethiol, dimethyl disulfide, diethyl
586 disulfide, dipropyl disulfide were equal to 0.0243, 0.06, 0.08, 0.96, 1.2 and 2.5 mM
587 respectively. The arrow indicates the incubation time used in tests with methanethiol. **B.**
588 Inhibition results for the second rate of the oxygen consumption rate. Concentrations of
589 methanethiol, ethanethiol, propanethiol, dimethyl disulfide, diethyl disulfide, dipropyl
590 disulfide were equal to 0.04, 0.01, 0.04, 0.1, 0.1 and 0.42 mM respectively. In all experiments
591 the biomass concentration was 10 mgN L^{-1}, $[Na^+ + K^+]$ = 1 M, pH = 9 and T = 35 °C.

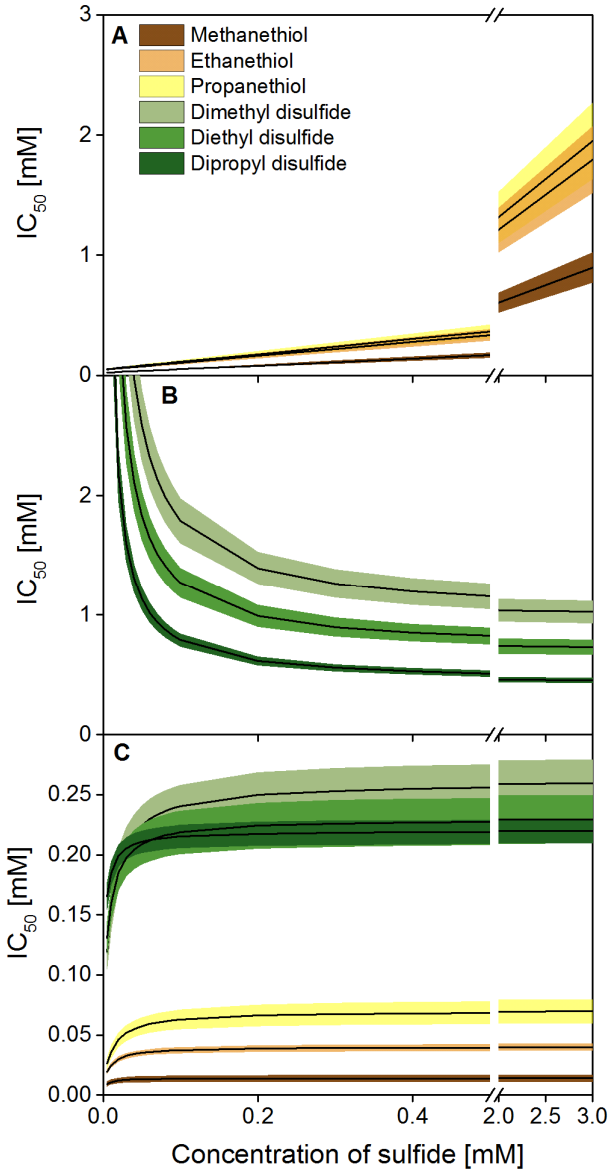

592

593 **Figure 3.** Calculated IC_{50} values with corresponding uncertainty bounds at increasing
594 concentration of sulfide. **A.** Methanethiol, ethanethiol and propanethiol for the first oxygen
595 consumption rate (R1). **B.** Dimethyl disulfide, diethyl disulfide and dipropyl disulfide (R1).
596 **C.** All aforementioned inhibitors for the second oxygen consumption rate (R2).

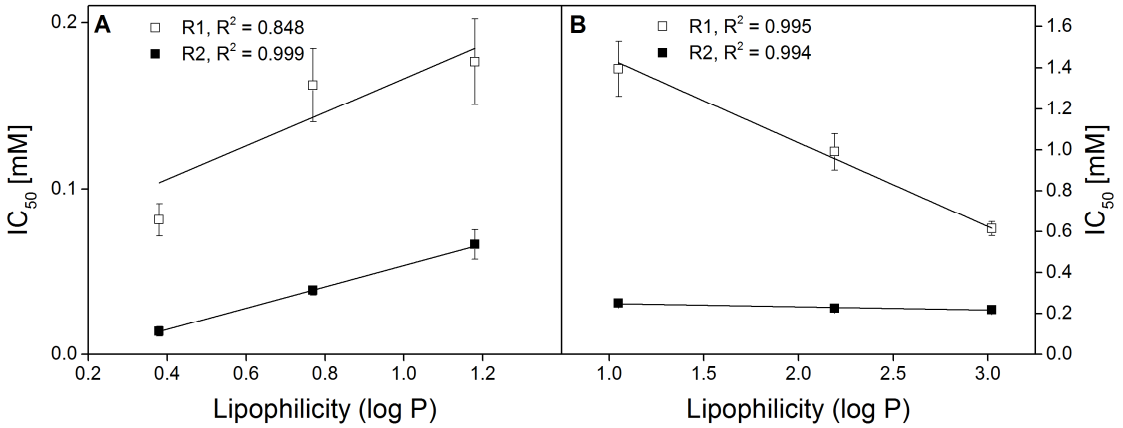

Figure 4. Relationship between lipophilicity and IC_{50} values at sulfide concentration of 0.2 mM. **A.** Methanethiol, ethanethiol, propanethiol for the first (R1) and the second (R2) oxygen consumption rate. **B.** Dimethyl disulfide, diethyl disulfide, dipropyl disulfide for R1 and R2.

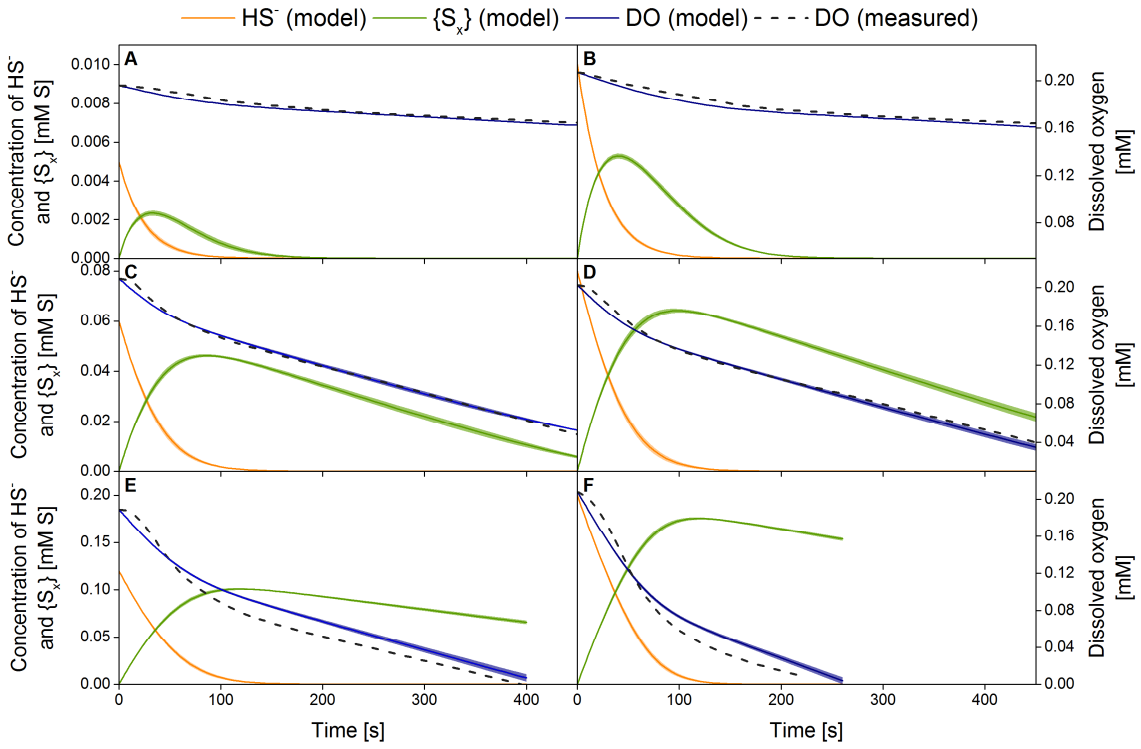

Figure 5. Comparison between measured and predicted dissolved oxygen (DO) consumption rate and model predictions of sulfide (HS^-) and polysulfur compound $\{S_x\}$ concentrations, in absence of an inhibitor. Results of the simulation are based on estimates from Table 3. The sample interval is 1 s for both measured and predicted results. The initial sulfide concentration was 0.005, 0.01, 0.06, 0.08, 0.12, 0.2 mM in figures A-F, respectively. The biomass concentration was 10 mgN L^{-1}, $[Na^+ + K^+]$ = 1 M, pH = 9 and T = 35 °C.

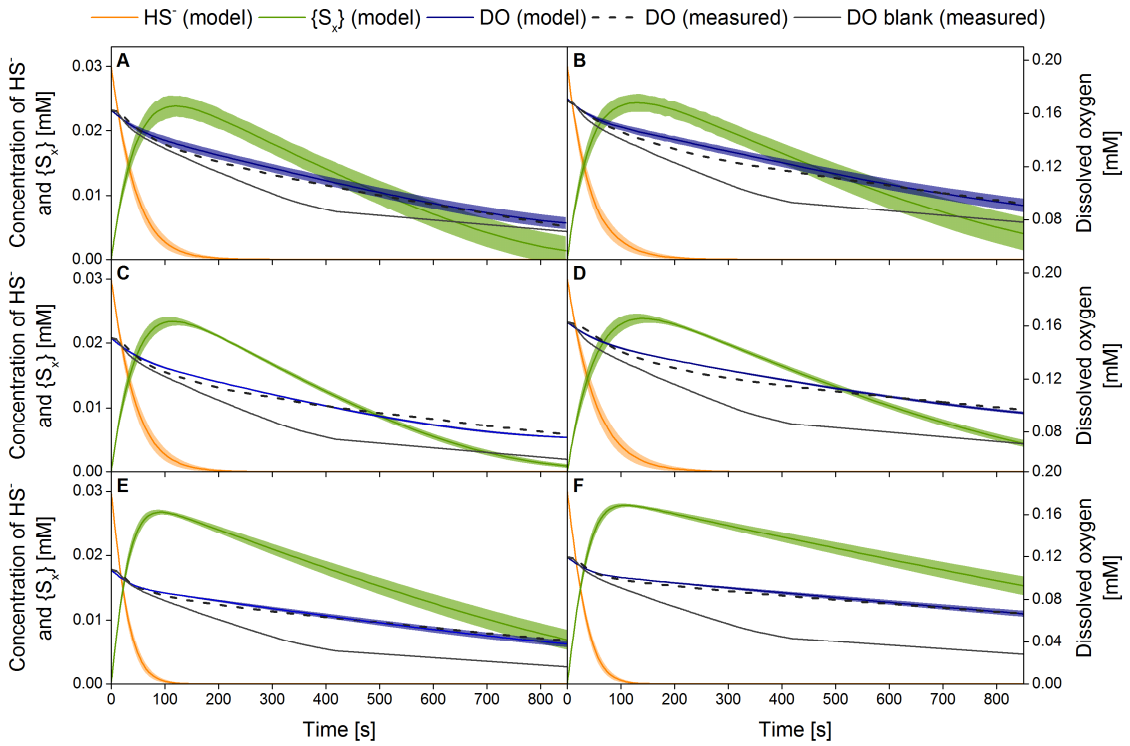

608

609 **Figure 6.** Comparison between measured and predicted dissolved oxygen (DO) consumption
610 rate and model predictions of sulfide (HS^-) and polysulfur compound $\{S_x\}$ concentration with
611 corresponding model output uncertainties as a result of variations in estimated parameters.
612 Results of the simulation are based on estimates from Table 3. The sample interval is 1 s for
613 both measured and predicted results. Respiration test were performed at different
614 concentration of various inhibitors: **A.** Methanethiol, 0.02 mM. **B.** Methanethiol, 0.04 mM. **C.**
615 Ethanethiol, 0.04 mM. **D.** Ethanethiol, 0.08 mM. **E.** Dimethyl disulfide, 0.5 mM. **F.** Dimethyl
616 disulfide, 1 mM. DO blank refers to an experiment performed without inhibitor. The biomass
617 concentration was 10 mgN L^{-1}, $[Na^+ + K^+]$ = 1 M, pH = 9 and T = 35 °C.

Supplementary Information

S1. Figures:

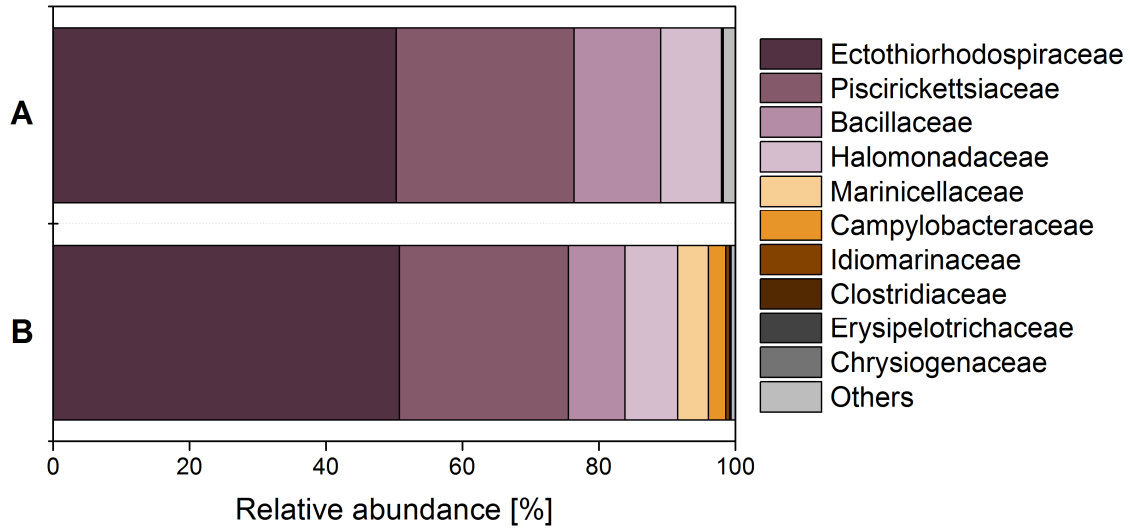

Figure S1. Relative abundance of the microbial composition based on the 16S rRNA gene for the biomass from a full-scale gas biodesulfurization installation (Janssen et al. 2009). Only bacteria with a relative abundance higher than 0.5% are listed (remaining bacteria are grouped into “Others”). A and B represents two replicates.

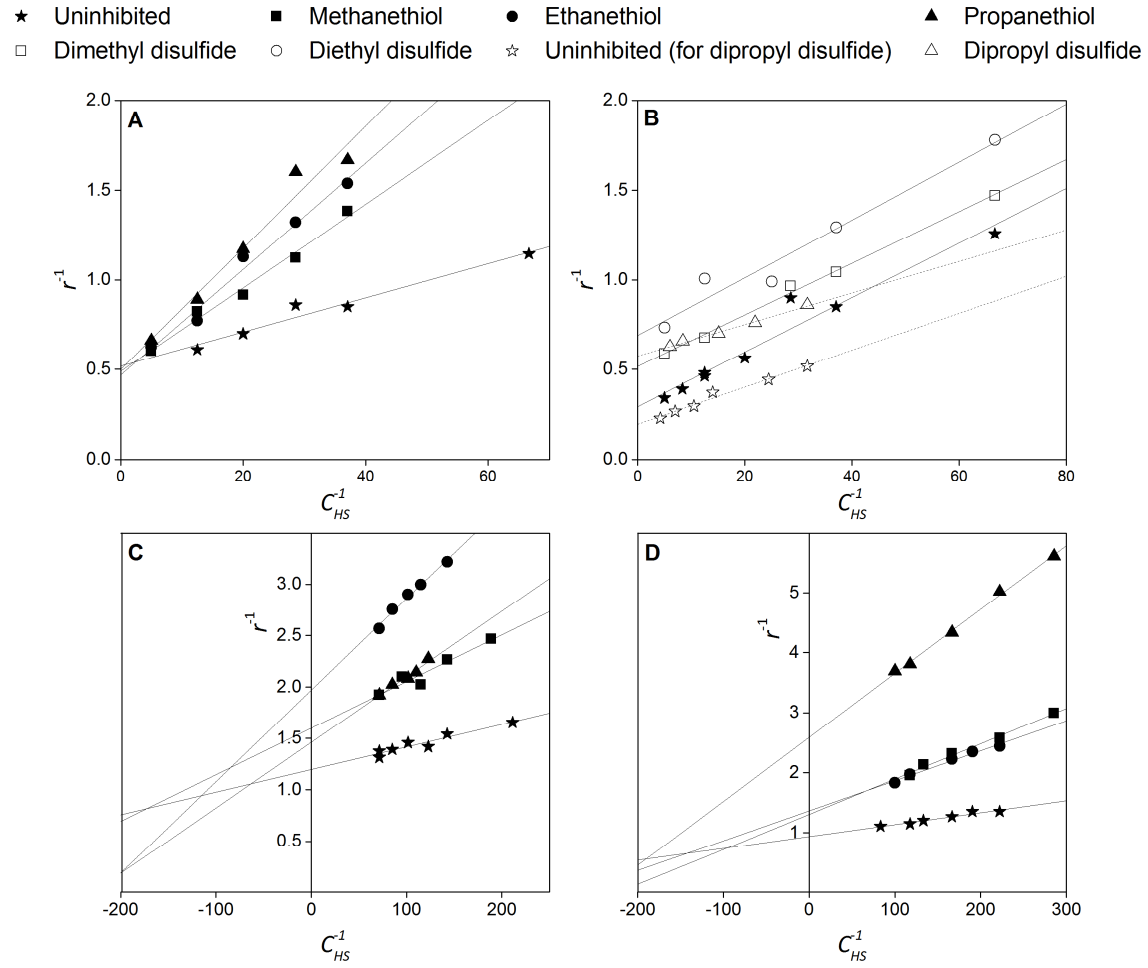

Figure S2. An example of results from sulfide-dependent respiration tests plotted on double-reciprocal plots for the first (A and B) and the second (C and D) oxygen consumption rate, where r is the reaction rate (mM O_2 (mg N h)$^{-1}$) and C_{HS} is the sulfide concentration (mM). The inhibitors concentrations for each oxygen consumption rate are given in Table 2. The biomass concentration was 10 mg N L^{-1}, pH = 9 and T = 35 °C.

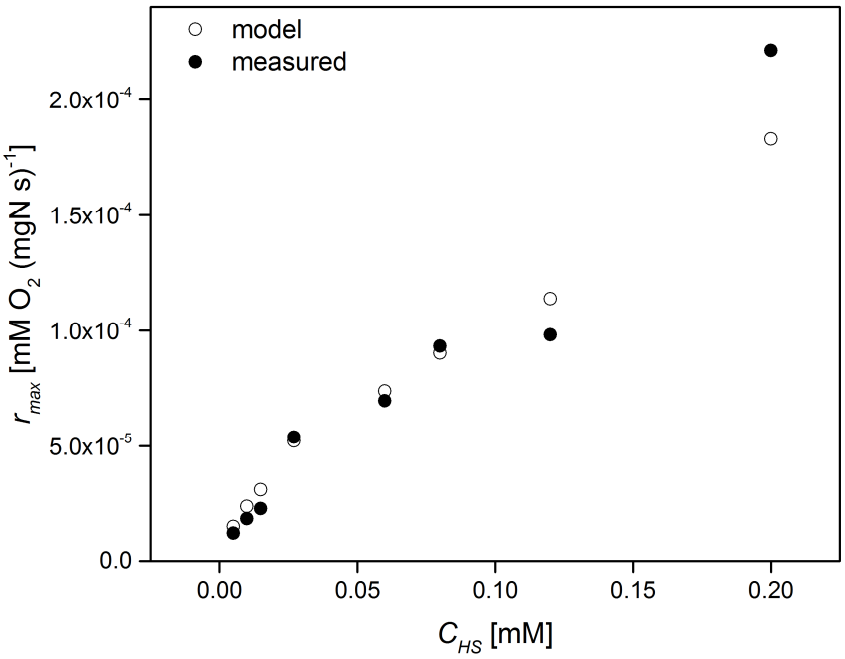

Figure S3. Comparison between measured and predicted reaction rate for the first rate of the oxygen consumption rate at different initial sulfide concentrations.

S2. Covariance and correlation matrix of the estimates

The parameter estimates related to the first oxygen consumption rate (R1) are given by:

$$\hat{\theta}_{R1} = \begin{pmatrix} r_{max}^{R1} \\ K_m^{R1} \end{pmatrix} = \begin{pmatrix} 0.6 \\ 0.079 \end{pmatrix}$$

with corresponding covariance and correlation matrices:

$$COV\hat{\theta}_{R1} = \begin{pmatrix} 0.0012 & 0.0003 \\ 0.0003 & 0.0001 \end{pmatrix}$$

$$R_{\hat{\theta}_{R1}} = \begin{pmatrix} 1 & 0.866 \\ 0.866 & 1 \end{pmatrix}$$

Similarly, parameters estimates related to the second oxygen consumption rate (R2) are described by:

$$\hat{\theta}_{R2} = \begin{pmatrix} r_{max}^{R2} \\ K_m^{R2} \end{pmatrix} = \begin{pmatrix} 0.103 \\ 0.0019 \end{pmatrix}$$

$$COV\hat{\theta}_{R2} = \begin{pmatrix} 0.0000148 & 0.0000019 \\ 0.0000019 & 0.0000003 \end{pmatrix}$$

$$R_{\hat{\theta}_{R2}} = \begin{pmatrix} 1 & 0.864 \\ 0.864 & 1 \end{pmatrix}$$